

Article

Observed Trends of Climate and River Discharge in Mongolia's Selenga Sub-Basin of the Lake Baikal Basin

Batsuren Dorjsuren ^{1,2}, Denghua Yan ^{1,3,4,*}, Hao Wang ^{1,3,4}, Sonomdagva Chonokhuu ², Altanbold Enkhbold ⁵, Xu Yiran ⁶, Abel Girma ^{1,7}, Mohammed Gedefaw ^{1,7} and Asaminew Abiyu ¹

¹ College of Environmental Science and Engineering, Donghua University, Shanghai 201620, China; Batsuren@seas.num.edu.mn (B.D.); Wanghao@iwhr.com (H.W.); Abelethiopia@yahoo.com (A.G.); Mohammedgedefaw@gmail.com (M.G.); Asaminewab@yahoo.com (A.A.)

² Department of Environment and Forest Engineering, School of Engineering and Applied Sciences, National University of Mongolia, Ulaanbaatar 210646, Mongolia; ch_sonomdagva@num.edu.mn

³ State Key Laboratory of Simulation and Regulation of Water Cycle in River Basin, China Institute of Water Resources and Hydropower Research (IWHR), Beijing 100038, China

⁴ Water Resources Department, China Institute of Water Resources and Hydropower Research (IWHR), Beijing 100038, China

⁵ Department of Geography, School of Art & Sciences, National University of Mongolia, Ulaanbaatar 210646, Mongolia; altanbold@num.edu.mn

⁶ School of Resources and Earth Science, China University of Mining and Technology, Xuzhou 221116, China; hsuijan@163.com

⁷ Department of Natural Resource Management, University of Gondar, Gondar 196, Ethiopia

* Correspondence: Yandh@iwhr.com; Tel.: +86-10-68781976

Received: 11 September 2018; Accepted: 9 October 2018; Published: 12 October 2018



Abstract: Mongolia's Selenga sub-basin of the Lake Baikal basin is spatially extensive, with pronounced environmental gradients driven primarily by precipitation and air temperature on broad scales. Therefore, it is an ideal region to examine the dynamics of the climate and the hydrological system. This study investigated the annual precipitation, air temperature, and river discharge variability at five selected stations of the sub-basin by using Mann-Kendall (MK), Innovative trend analysis method (ITAM), and Sen's slope estimator test. The result showed that the trend of annual precipitation was slightly increasing in Ulaanbaatar ($Z = 0.71$), Erdenet ($Z = 0.13$), and Tsetserleg ($Z = 0.26$) stations. Whereas Murun ($Z = 2.45$) and Sukhbaatar ($Z = 1.06$) stations showed a significant increasing trend. And also, the trend of annual air temperature in Ulaanbaatar ($Z = 5.88$), Erdenet ($Z = 3.87$), Tsetserleg ($Z = 4.38$), Murun ($Z = 4.77$), and Sukhbaatar ($Z = 2.85$) was sharply increased. The average air temperature has significantly increased by $1.4\text{ }^{\circ}\text{C}$ in the past 38 years. This is very high in the semi-arid zone of central Asia. The river discharge showed a significantly decreasing trend during the study period years. It has been apparent since 1995. The findings of this paper could help researchers to understand the annual variability of precipitation, air temperature, and river discharge over the study region and, therefore, become a foundation for further studies.

Keywords: precipitation; air temperature; river discharge; Mann-Kendall test; Selenga river basin; Lake Baikal basin; Mongolia

1. Introduction

The Lake Baikal basin (LBB) is a suitable area to study climate change impacts. The climate is a long-term prevailing weather condition. Weather parameters include air temperature, precipitation,

humidity, sunshine hours, cloudiness, atmospheric pressure, the number of rainy days, wind velocity, etc. These parameters interact directly or indirectly, greatly affecting the environment and the living organisms [1]. The semi-arid environment is highly vulnerable to climate change [2,3]. Land surface temperature is an important ecological factor and its warming trend will influence the topsoil [4,5]. Evapotranspiration and precipitation rates may change due to changes in soil temperature and air temperature.

Precipitation change may greatly affect the hydrological system of the basin. Due to climate change and intensive human activities in recent decades, the runoff of many rivers in the world has been changing. About 22% of the world's rivers were shown to have a significant decrease in the annual runoff because of increasing water consumptions and diversion [6,7].

The most sensitive areas for climate change are arid and semi-arid regions of central Asia [2,8,9]. LBB is the largest representative of these regions [3,10]. Lake Baikal, as the world's largest natural freshwater lake and its corresponding catchments, is already affected by climate change and the water quantity becomes erratic [10]. In recent decades, changes in hydrological and water quantity are primarily attributed to climate change, land use change, contaminant influx from mining areas and urban settlements as well [11].

As the largest sub-basin of LBB, Selenga River basin is located in the Mongolian and Russian Federation. The Mongolian plateau is spatially extensive, with pronounced environmental gradients driven primarily by precipitation and air temperature on large scales. Therefore, it is an ideal region to examine the dynamics of the landscape structures and hydrology parameters [9]. This area, hydro-climatic changes can also lead to a shift in hydrology parameters, ecosystem and lake conditions in these areas. In addition, human activity effects on water pollution, water resources, sedimentary, and river discharge. In particular, in the Mongolian's Selenga River basin high socio-economic activities are taking place. In the study region, there is high population density particularly, around Tuul and Kharaa sub basin. The sub basin is located in the biggest cities of Mongolia (Ulaanbaatar, Darkhan, and Erdenet), thus the river basin is highly consumed by the city residence. They consumed the water for agriculture, recreation and domestic use. In addition, the Selenga river basin water resource is used by the mining industry. Thus, it has a great role in reducing the quantity of the basin water flow [3,11,12].

This paper aims to investigate spatial and temporal changes in climate and river discharge changes in Mongolia's Selenga sub-basin of the LBB understanding from 1979 to 2016. The overall objectives of the present study are (i) to identify historical climate trends, (ii) to identify trends of spatial and temporal changes in the river discharge, (iii) to assess the relationship and to which extent can climate change trends affect the river discharge.

2. Materials and Methods

2.1. Study Area

Lake Baikal is the oldest (about 25 million years old), deepest (1637 m) and largest freshwater lake (23,000 km³) and is located in the southern part of East Siberia [13]. The transboundary basin of Lake Baikal is located on the boundary of North and Central Asia (96°52'–113°50' N, 46°28'–56°42' W) [12]. The longest stretch of the basin from southwest to north-east is 1470 km, and from west to east is 962 km. The minimal length from west to east is 193 km (Figure 1). The total area of the basin is 573,478 km², and 52% of which belong to Mongolia and the remaining belongs to the Russian Federation [14]. In recognition of its biodiversity and endemism, United Nations Educational, Scientific and Cultural Organization (UNESCO) declared Lake Baikal as a World Heritage Site in 1996. The lake contains an outstanding variety of endemic flora and fauna, which is an exceptional value to evolutionary science. It is also surrounded by a system of protected areas with good scenery and natural values [10,15,16].

As the largest sub-basin of LBB, Selenga River basin is located in the Mongolian and Russian Federation. The Selenga is a Trans-boundary river, the largest tributary of Lake Baikal. On the average, it discharges into Lake Baikal ~30 km³ of water, i.e., half of the total inflow into the lake.

Forty-six percent of Selenga annual runoff forms in Mongolian territory. The Mongolian plateau is spatially extensive, with pronounced environmental gradients driven primarily by precipitation and air temperature on large scales. The length of the river is 1024 km, its drainage area is 447.06 thousand km², of which 148.06 thousand km² are in the territory of Russia.

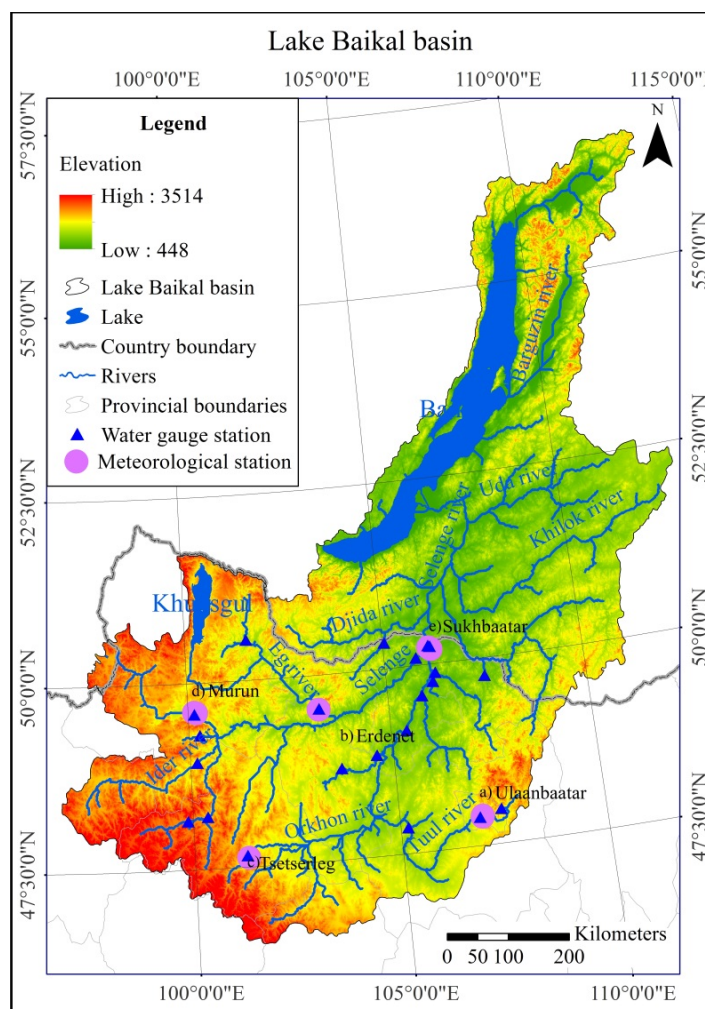


Figure 1. Location of Lake Baikal basin (LBB), Water gauge station and meteorological stations of the Selenga River basin located in the Mongolian.

2.2. Data Sources

The data of air temperature, precipitation and hydrologic data of in Mongolia's Selenga river basin were taken from Information and Research Institute of Meteorology, Hydrology, and Environment (IRIMHE) hosts (<http://irimhe.namem.gov.mn/>), and National Centers for Environmental Information NOAA's National Centers for Environmental Information (NCEI) hosts (<https://ngdc.noaa.gov/>). The location of the 5 water gauge stations used in this study is shown in Figure 1. For the selection of climate and water gauge stations in Mongolia's Selenga sub-basin of the LBB, the following factors were taken into consideration: (1) spatial distribution; (2) capacity of stations and (3) whether it is near to the water system (Figure 1) [8,17].

2.3. Methods

Analyses of long-term trends in both the observed and adjusted data were done using the Mann-Kendall test, with linear changes in the data represented by Kendall-Theil Robust Lines. This non-parametric approach is well suited for evaluating changes in hydrologic regimes.

The appendix of [18] provides a concise explanation of the statistics as applied to river discharge data [19], to remove the influence of serial correlations on the trend analyses. Trend analysis is used to investigate whether the trend is upward, downward, or no trend in data value points. The non-parametric Mann-Kendall (MK) test has been applied in studies to detect the trends in hydro-meteorological observations that do not need the normal distribution of data points. This paper used the Mann-Kendall (MK) test method to detect the trends in climate and river discharge time series data. To evaluate the reliability of Mann-Kendall (MK), the results were compared with ITAM and Sen’s slope estimator test. In addition, annual and seasonal precipitation variability time series data were investigated by statistical analysis. The study region has four distinct seasons: summer (June–August), autumn (September–November), winter (December–February) and spring (March–May). Significance levels at 10%, 5%, and 1% were taken to assess the climate and river discharge time’s series data by MK, ITAM, and Sen’s slope estimator method (Figure 2).

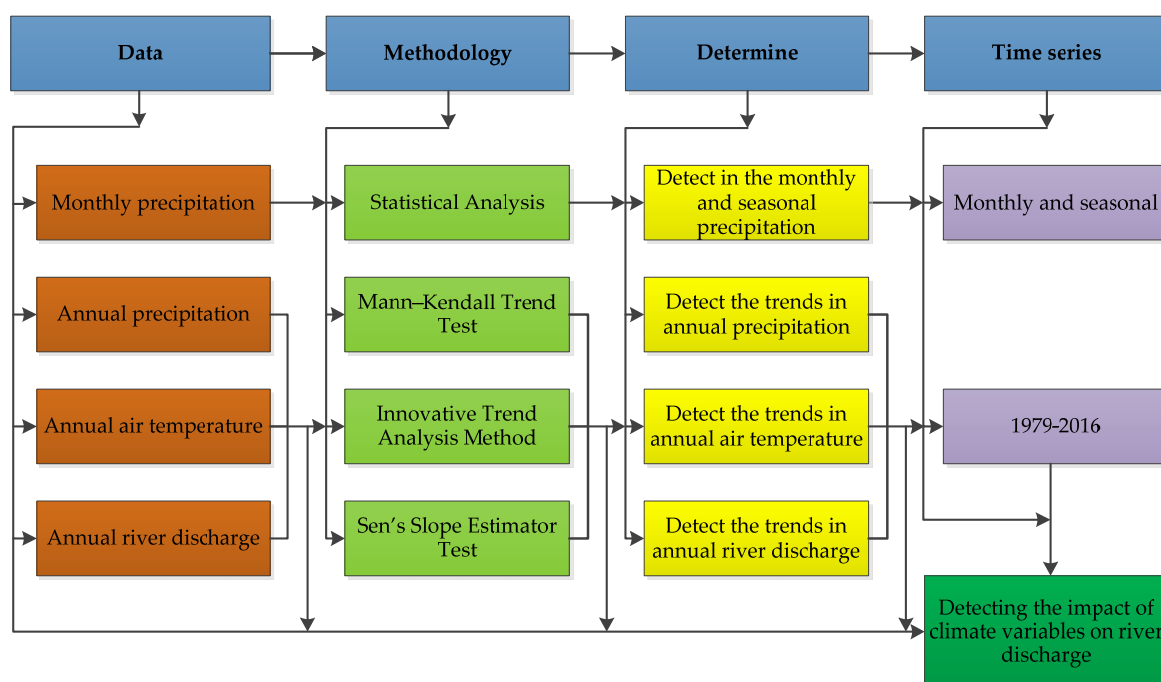


Figure 2. Workflow diagram to detect the changing trends in hydro-meteorological.

2.3.1. Mann-Kendall Trend Test

The Mann-Kendall (MK) test method also shows upward and downward trends with statistical significance. The strength of the trend depends on the magnitude, sample size, and variations of data series. The trends in the MK test is not significantly affected by the outliers occurred in the data series since the MK test statistic depends on positive or negative signs [20–22].

Annual and seasonal data series are used for trend analysis in this study. The trends of annual precipitation, air temperature, and river discharge have been also analyzed separately.

Individual time series data of climate and discharge are compared with all corresponding time series data of the year. When the data point of later year is larger than the data point of the previous year, the MK statistics is increased by one otherwise the MK statistics decreased by one. Thus, the MK statistics is the cumulative result of all the data values. The Mann-Kendall test statistics “S” is then equated as:

$$S = \sum_{i=1}^{n-1} \sum_{j=i+1}^n \text{sgn} (x_j - x_i) \tag{1}$$

The trend test is applied to x_i data values ($i = 1, 2, \dots, n - 1$) and x_j ($j = i + 1, 2, \dots, n$). The data value of each x_i is used as a reference point to compare with the data value of x_j which is given as:

$$\text{sgn}(x_j - x_i) = \begin{cases} +1 & \text{if } (x_j - x_i) > 0 \\ 0 & \text{if } (x_j - x_i) = 0 \\ -1 & \text{if } (x_j - x_i) < 0 \end{cases} \quad (2)$$

where x_j and x_i are the values in period j and i . When the number of data series greater than or equal to ten ($n \geq 10$), MK test is then characterized by a normal distribution with the mean $E(S) = 0$ and variance $Var(S)$ is equated as [23]:

$$E(S) = 0 \quad (3)$$

$$Var(S) = \frac{n(n-1)(2n+5) - \sum_{k=1}^m t_k(t_k-1)(2t_k+5)}{18} \quad (4)$$

where m is the number of the tied groups in the time series, and t_k is the number of ties in the k th tied group.

The test statistics Z is as follows:

$$Z = \begin{cases} \frac{s-1}{\delta} & \text{if } S > 0 \\ 0, & \text{if } S = 0 \\ \frac{s+1}{\delta} & \text{if } S < 0 \end{cases} \quad (5)$$

when Z is greater than zero, it indicates an increasing trend and when Z is less than zero, it is a decreasing trend.

In time sequence, the statistics are defined independently:

$$UF_k = \frac{d_k - E(d_k)}{\sqrt{var(d_k)}} \quad (k = 1, 2, \dots, n) \quad (6)$$

Firstly, given the confidence level α , if the $UF_k > UF_\alpha/2$, indicates that the sequence has the significant trend. Then, the time sequence is arranged in reverse order. According to the equation calculation, while making

$$UB_k = -UF_k \quad (7)$$

$$K = n + 1 - k \quad (8)$$

Finally, UB_k and UF_k are drawn as UB and UF curve. If there is an intersection between the two curves, the intersection is the beginning of the mutation [24].

2.3.2. Innovative Trend Analysis Method (ITAM)

Innovative trend analysis method (ITAM) has been used in many studies to detect the hydrometeorological observations and its accuracy was compared with the results of MK method [25,26]. The ITAM divides a time series into two equal parts, and it sorts both sub-series in ascending order. Then after, the two halves placed on a coordinate system ($x_i : i = 1, 2, 3, \dots, n/2$) on X-axis and ($x_j : j = n/2 + 1, n/2 + 2, \dots, n$) on Y-axis. If the time series data on a scattered plot are collected on the 1:1 (45°) straight line, it indicates no trend. However, the trend is increasing when data points accumulate above the 1:1 straight line and decreasing trend when data points accumulate below the 1:1 straight line.

The mean value difference between x_i and x_j could give the trend magnitude of data series. The first observed data point was not considered in this study when classifying the time series data into x_i and x_j data plots since the total number of observed data points are 38 from 1979–2016.

The direction of the trend is also affected by x_i data series. The trend indicator of ITAM is multiplied by 10 to make the scale similar to the other two tests. The trend indicator is given as:

$$\phi = \frac{1}{n} \sum_{i=1}^n \frac{10(x_j - x_i)}{\mu} \quad (9)$$

where ϕ = trend indicator, n = number of observation on the subseries, x_i = data series in the first half subseries class, x_j = data series in the second half subseries part and μ = mean of data series in the first half subseries part.

A positive value of ϕ indicates an increasing trend. However, a negative value of ϕ indicates a decreasing trend. However, when the scatter points closest around the 1:1 straight line, it implies the non-existence of a significant trend.

2.3.3. Sen's Slope Estimator Test

The trend magnitude is calculated by [27–30] slope estimator methods. The slope Q_i between two data points is given by the equation:

$$Q_i = \frac{x_j - x_k}{j - k}, \text{ for } i = 1, 2, \dots, N \quad (10)$$

where x_j and x_k are data points at time j and ($j > k$), respectively. When there is only single datum in each time, then $N = \frac{n(n-1)}{2}$; n is number of time periods. However, if the number of data in each year is many, then $N < \frac{n(n-1)}{2}$; n total number of observations. The N values of slope estimator are arranged from smallest to biggest. Then, the median of slope (β) is computed as:

$$\beta = \begin{cases} Q[(N+1)/2] & \text{when } N \text{ is odd} \\ Q[(N/2) + Q(N+2)/(2)/(2)] & \text{when } N \text{ is even} \end{cases} \quad (11)$$

The sign of β shown whether the trend is increasing or decreasing.

3. Results

3.1. Analysis of Precipitation

Annual mean precipitation of the study region from 1979 to 2016 was found to be 295.2 mm. The minimum and maximum recorded annual average precipitations were 175.0 and 380.0 mm respectively. The seasons of the study region are divided into four categories: Spring, summer, autumn, and winter seasons. The summer season has the largest proportion of precipitation. The seasonal precipitation varied from spring 39.27 mm (13.3%) to Summer 204.11 mm (69.15%), autumn 43.51mm (14.74%) to Winter 8.29 mm (2.81%) (Table 1).

The MK curve annual precipitation (changing parameters) shows a sharp decreasing trend in Ulaanbaatar 1994 to 2010 ($Z = 0.71$), a sharp decreasing trend in Erdenet from 1994 to 2005 ($Z = 0.13$), also, a sharp decreasing trend in Tsetserleg from 1994 to 2005 ($Z = 0.26$), a statistically significant increasing trend in Murun from 1984 to 1995 ($Z = 2.45$), in Sukhbaatar a significant increasing trend was observed with ($Z = 1.06$) from 1981 to 2016 and finally a statistically significant increasing trend was observed in Average (five stations) from 1984 to 1987 ($Z = 0.68$) (Figure 3).

The annual trend analysis of precipitation in all station using the Mann Kendall test, ITAM, Sen's slope estimator test result are presented in (Table 2). The trend in ITAM test shows an increasing trend in Murun and decreasing trend in other stations. Hence, the increase and decrease in innovative trend analysis ϕ test value predict that the magnitude becomes strong and weak, respectively.

Table 1. The monthly and seasonal precipitation of stations.

Months, Season	Ulaanbaatar (mm)	Erdenet (mm)	Tsetserleg (mm)	Murun (mm)	Sukhbaatar (mm)	Average Precipitation (mm)	Z-Score
January	2.38	2.54	2.52	1.47	3.09	2.40	(−0.83)
February	2.45	2.56	2.90	1.10	2.18	2.24	(−0.84)
March	4.60	6.93	7.37	1.40	2.66	4.59	(−0.75)
April	8.39	14.03	13.47	7.71	9.74	10.67	(−0.52)
May	20.53	24.13	32.52	17.89	24.98	24.01	(−0.02)
June	48.23	69.73	58.95	48.19	48.78	54.78	1.13
July	69.37	99.39	86.13	69.86	64.01	77.75	1.99
August	66.80	86.26	75.71	57.60	71.55	71.58	1.76
September	25.52	34.71	25.98	19.78	32.45	27.69	0.12
October	8.94	12.34	13.07	5.62	10.02	10.00	(−0.55)
November	5.48	7.61	6.27	3.06	6.73	5.83	(−0.70)
December	3.52	4.28	3.02	2.98	4.44	3.65	(−0.79)
Spring	33.52	45.09	53.36	26.99	37.38	39.27 (13.3%)	0.55
Summer	184.41	255.38	220.79	175.65	184.34	204.11 (69.15%)	6.73
Autumn	39.94	54.66	45.31	28.46	49.20	43.51 (14.74%)	0.71
Winter	8.35	9.39	8.43	5.56	9.71	8.29 (2.81%)	(−0.61)
Annual precipitation	266.22	364.52	327.89	236.66	280.62	295.18 (100%)	10.14

Note: The number in the brackets indicates low precipitation rates.

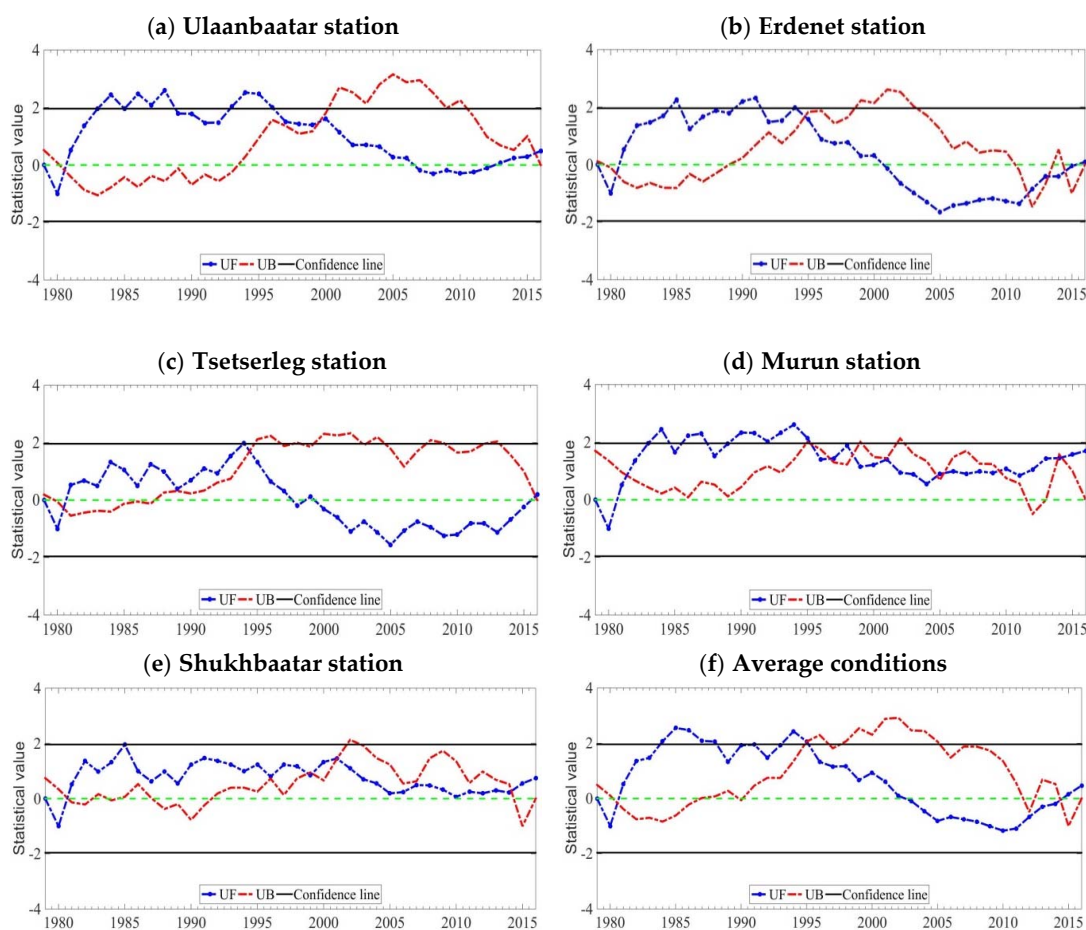


Figure 3. Trends of annual precipitation across stations (note: UF and UB are changing parameters where $UB = -UF$).

Table 2. The result of Z-statistic of Mann-Kendall (MK), Innovative Trend Analysis Method (ITAM) (ϕ), and Sen’s slope estimator test (β).

S/No.	Name of Stations	Z (MK)	ϕ	β
1	Ulaanbaatar	0.71	−0.53	0.63
2	Erdenet	0.13	−0.41	0.28
3	Tsetserleg	0.26	−0.49	0.13
4	Murun	2.45 **	0.25	1.21 *
5	Sukhbaatar	1.06 *	−0.03	0.62
6	Average	0.68	−0.28	0.31

* Trends at 0.1 significance level; ** Trends at 0.05 significance level.

3.2. Analysis of Air Temperature

The MK curve annual air temperature (changing parameters) shows a statistically sharply increasing trend in Ulaanbaatar from 1994 to 2016 ($Z = 5.88$), a statistically sharp increasing trend in Erdenet from 1988 to 2016 ($Z = 3.87$), a statistically sharply increasing trend in Tsetserleg from 1993 to 2016 ($Z = 4.38$), a statistically sharp increasing trend in Murun from 1992 to 2016 ($Z = 4.77$), in Sukhbaatar a statistically significant increasing trend was observed with ($Z = 2.85$) from 1986 to 2013 and finally a statistically significant increasing trend was observed in Average (five stations) ($Z = 4.71$) (Figure 4).

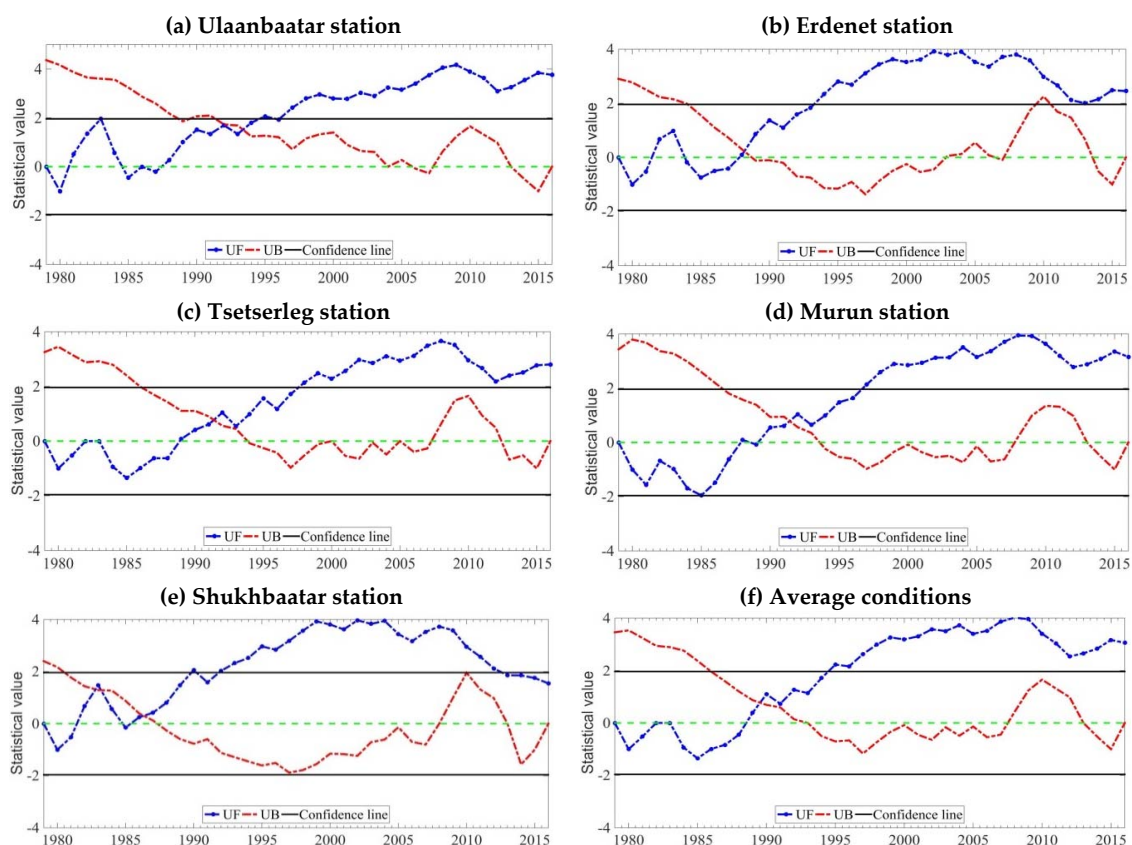


Figure 4. Trends of annual air temperature across stations (note: UF and UB are changing parameters where $UB = -UF$).

The annual trend analysis of air temperature in all station using the Mann Kendall test, ITAM, Sen’s slope estimator test result is presented in (Table 3). The trend in ITAM test shows an increasing trend in all stations. Hence, the increase and decrease in innovative trend analysis ϕ test value predict that the magnitude becomes strong.

Table 3. The result of Z-statistic of MK, ITAM (ϕ), and Sen’s slope estimator test (β).

S/No.	Name of Stations	Z (MK)	Φ	β
1	Ulaanbaatar	5.88 ***	−54.55 ***	0.05
2	Erdenet	3.87 ***	8.39 **	0.03
3	Tsetserleg	4.38 ***	7.26	0.04
4	Murun	4.77 ***	−47.56	0.06
5	Sukhbaatar	2.85 **	7.13 ***	0.02
6	Average	4.71 ***	18.66 ***	0.04

** Trends at 0.05 significance level; *** Trends at 0.01 significance level.

3.3. Analysis of River Discharge

The MK curve annual river discharge (changing parameters) shows a sharply decreasing trend in Ulaanbaatar 1994 to 2016 ($Z = -3.32$), a statistically sharp decreasing trend in Tsetserleg from 1982 to 2016 ($Z = -3.84$), a significant decreasing trend in Murun from 1986 to 2016 ($Z = -1.28$), in Sukhbaatar a significant decreasing trend was observed with ($Z = -2.05$) from 1993 to 2016 and finally a significant decreasing trend was observed in Average (five stations) ($Z = -2.05$) (Figure 5). The annual trend analysis of river discharge in all station using the Mann Kendall test, ITAM, Sen’s slope estimator test result are presented in (Table 4). The trend in ITAM test shows a decreasing trend in all stations. Hence, the increase and decrease in innovative trend analysis ϕ test value predict that the magnitude becomes strong.

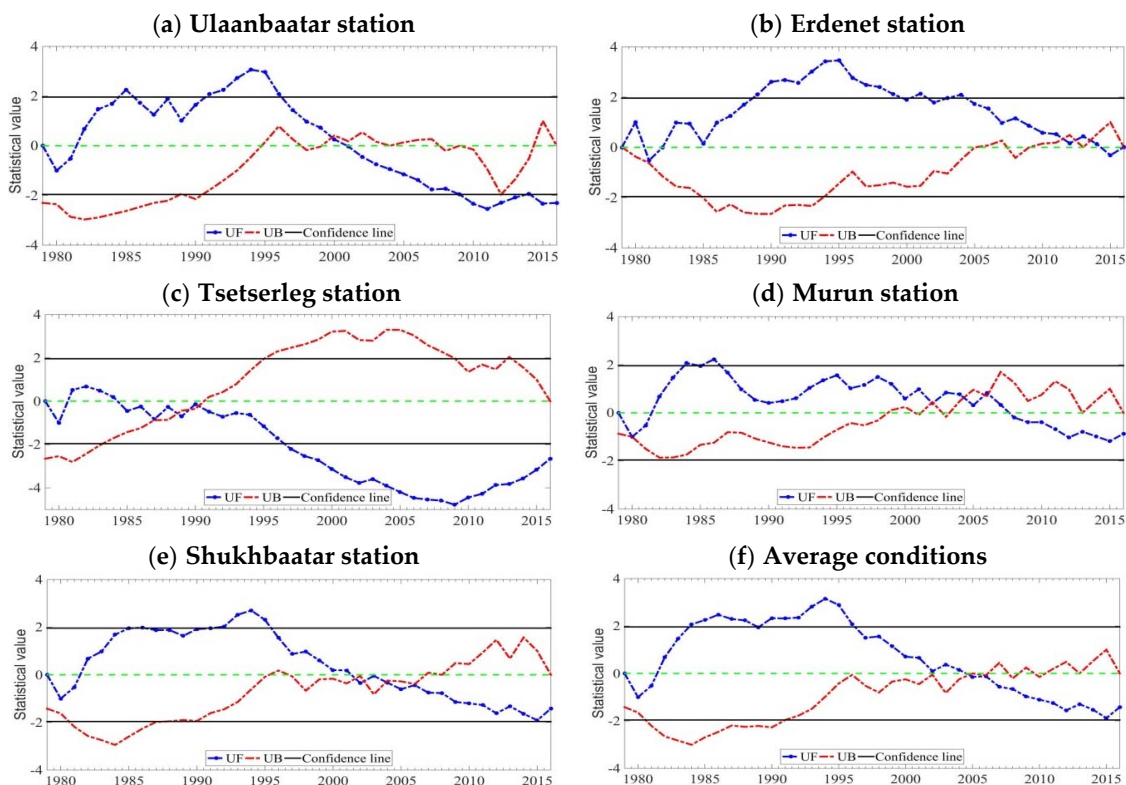


Figure 5. Trends of annual discharge across stations (note: UF and UB are changing parameters where $UB = -UF$).

Table 4. The result of Z-statistic of MK, ITAM (ϕ), and Sen’s slope estimator test (β).

S/No.	Name of Stations	Z (MK)	Φ	β
1	Ulaanbaatar	−3.32 ***	−5.63	−144.12
2	Erdenet	0.00	−0.96	4.46
3	Tsetserleg	−3.84 ***	−4.65	−56.31
4	Murun	−1.28 *	−1.01	−64.15
5	Sukhbaatar	−2.05 **	−2.00	−550.33
6	Average	−2.05 **	−2.00	−169.80

* Trends at 0.1 significance level; ** Trends at 0.05 significance level; *** Trends at 0.01 significance level.

River discharge trend is generally exhibited a downward trend from 1979 to 2016. Especially, river discharges show a sharp decreasing trend in all stations since 1995.

3.4. Relationship of Climate and River Discharge

The annual average air temperature of the study region from 1979 to 2016 was found to be 0.83 °C. The minimum and the maximum recorded air temperature were −0.9 °C and 2.9 °C per year, respectively. A dramatic increase in air temperature was observed from 1984 to 2007. In the study region, the observed air temperature was increased from 1979 to 2016 ($R^2 = 0.2632$) (Figure 6f). The warmest year was in 2007 (2.9 °C). The air temperature most increasing area is Ulaanbaatar city, it was increasing 1.9 °C ($R^2 = 0.4226$) (Figure 6a). The annual average air temperature increased significantly by 1.4 °C. The mean annual air temperature is 16 °C to 18 °C in July and −16 °C to −22 °C in January. In the Mongolian’s Selenga river basin, precipitation varies both in time and space scale. The average precipitation is 295.2 mm/year. About 85% of the total precipitation falls from April to September, of which about 69.15% falls during June, July and August. The air temperature and precipitation changes within the five stations show a different value (Figure 6). Overall precipitation showed a slightly increasing trend during the period from 1979 to 2016 (Figure 6f).

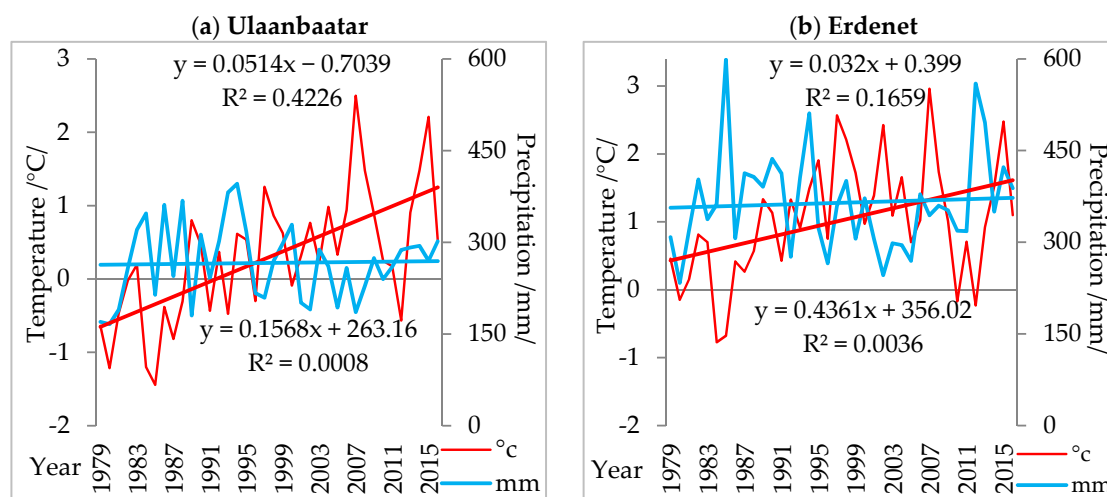


Figure 6. Cont.

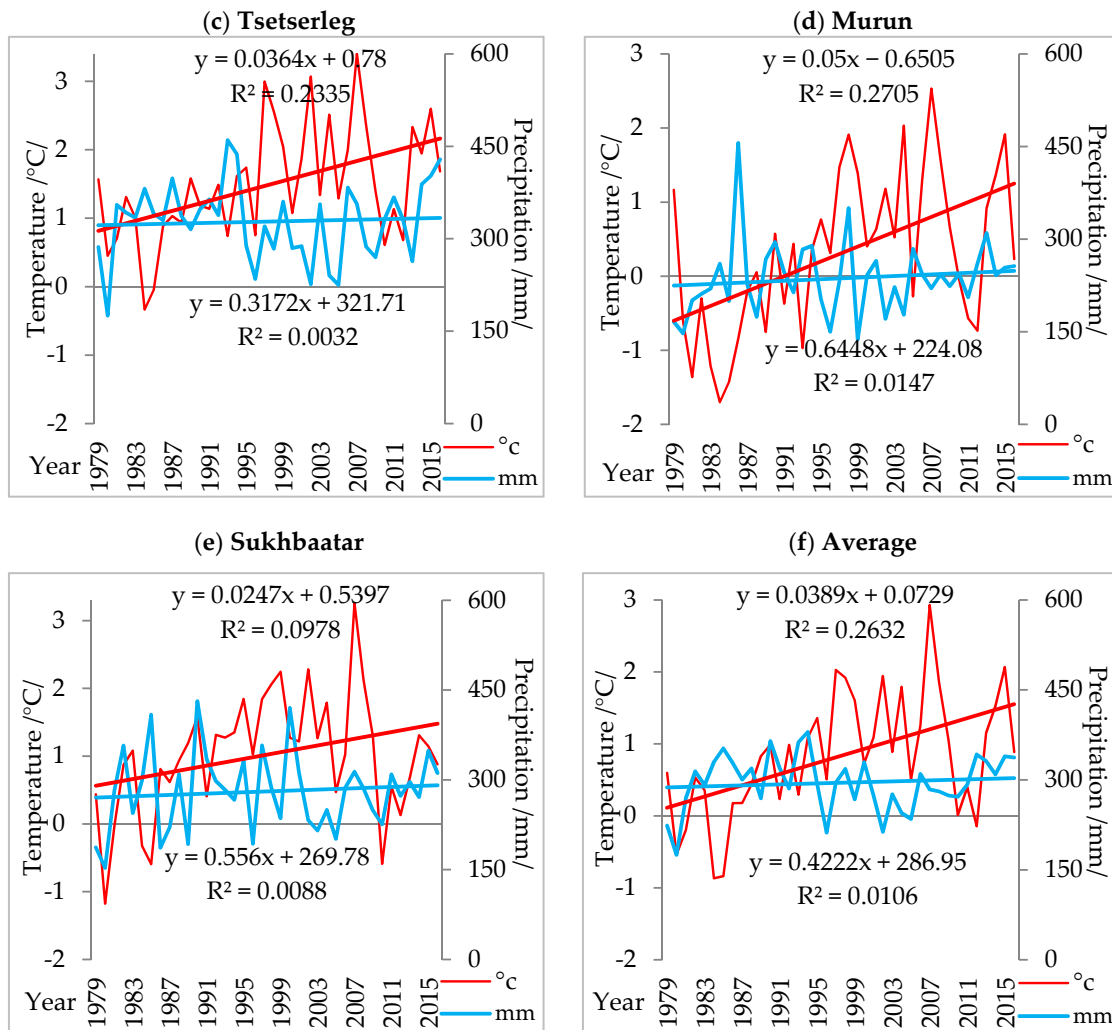


Figure 6. The air temperature and precipitation trend for the period 1979–2016. The vertical column is air temperature and precipitation change, and fluctuations line indicates annual values and solid lines indicate period running averages.

The ratio of precipitation and river discharge to this basin is calculated by the location of the five meteorological stations and water gauge stations (Figure 7). However, precipitation has been relatively stable ranging from 1979 to 2016 (Figure 7f).

The trend of air temperature change and the trend of river discharge were estimated. A statistically significant increase in average air temperature (five stations average) was from 1994 to 2016 ($Z = 4.71$). Also, the air temperature increased on all meteorological stations. River discharge exhibited a decreasing pattern (Figure 8).

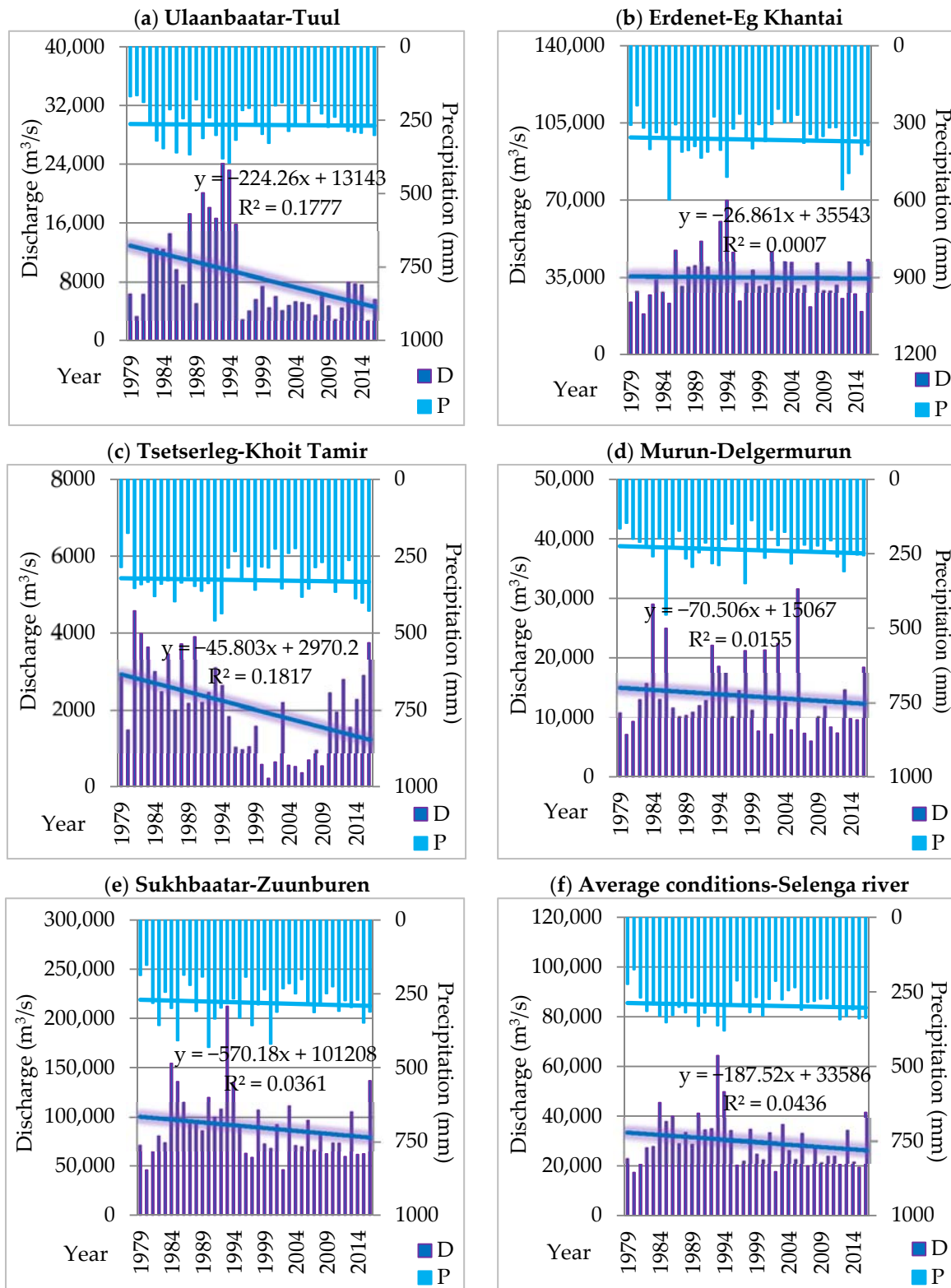


Figure 7. Long-term in precipitation and discharge change, in during 1979–2016.

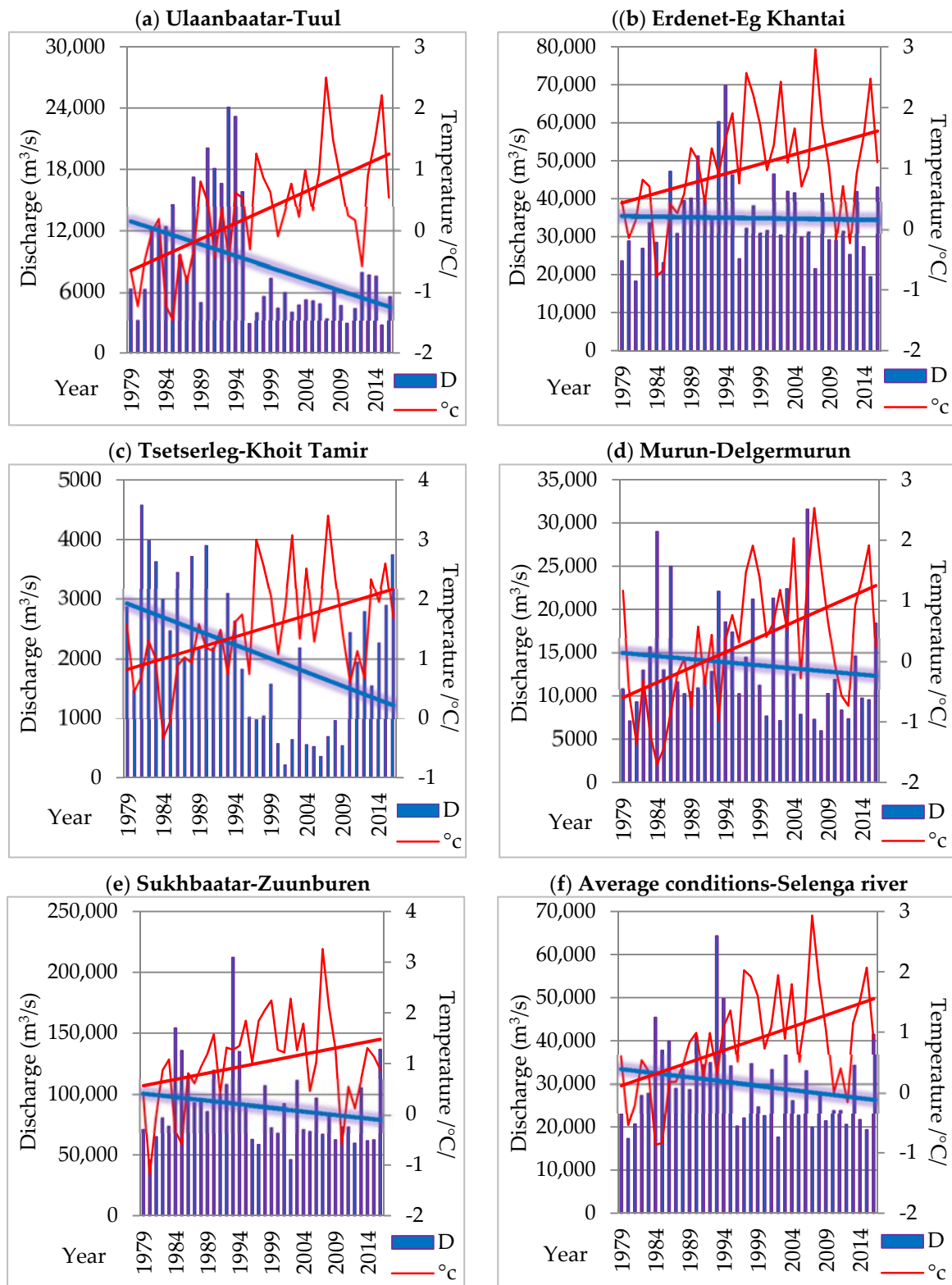


Figure 8. Long-term in air temperature and discharge change, in during 1979–2016.

Potential linkages between climate variables and the observed changes in river discharge are the subject of ongoing debate. To determine this, it was the estimation of the relationship between climate parameters and river discharge (Figure 9).

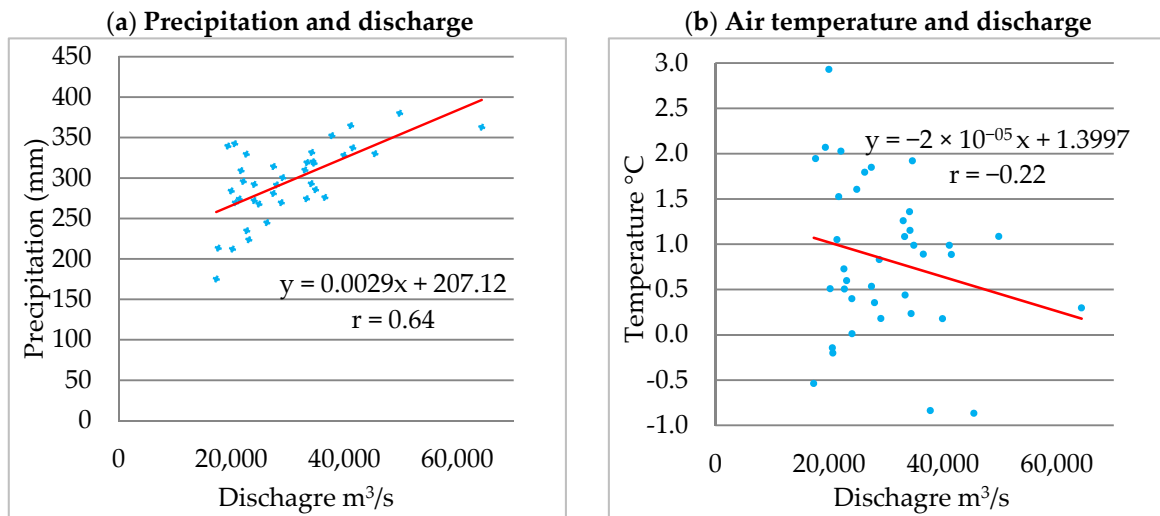


Figure 9. Correlation coefficient: climate and river discharge.

The correlation coefficient between precipitation and river discharge has a strong positive correlation ($r = 0.64$) from 1979 to 2016. In this case, the volume of the river discharge will increase when the number of precipitation increases. During this period, precipitation has increased. The correlation coefficient between air temperature and river discharge has a weak negative relationship ($r = -0.22$) from 1979 to 2016. In this case, the volume of the river discharge will decrease when the air temperature increases. However, Figures 7 and 8 shows that the river discharge has a sharp decreasing trend significantly since 1995, it may be related to the impact of other factors. During this period, quantities of the river discharge passing through bigger cities are dramatically decreasing. Climate change and river discharges are interdependent [31]. Especially in the rivers fed by precipitation, precipitation can directly affect the hydrological changes in the basin. Changes in river discharge are different at the five stations. In particular, River discharge decreased at the Tuul river water gauge station in Ulaanbaatar city. It has been decreased apparently since 1995. The water shortage was ($y = -224.26x + 13,143$). Also, The River discharge has been decreased in Zuunburen station near Sukhbaatar city. The water shortage was ($y = -570.18x + 101,208$). This may be due to the high consumption of the river water (Figure 7).

The average change in climate and river discharge was categorized by 10 years period. These include: from 1979 to 1988 (I), from 1989 to 1998 (II), from 1999 to 2008 (III), from 2009 to 2016 (IV) (Figure 10). During the III period, precipitation decreases, the temperature increases and also the river discharge decrease this is in illustrated in Figure 9.

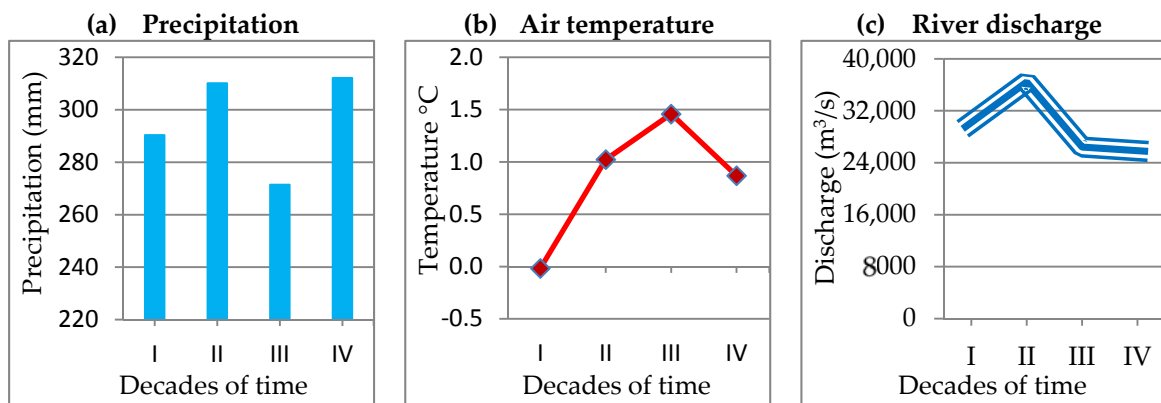


Figure 10. Decades changing of climate and river discharge.

However, during in period IV, the amount of precipitation increased, the air temperature decreased, and the river discharge also decreased. This could be related to other factors rather than climatic factors.

4. Discussion

An increase in air temperature is among the manifestations of global climate change. The global average air temperature has increased by 0.85 °C from 1880 to 2012, and this may even accelerate in the near future. The air temperature of worldwide large inland water bodies has been rapidly warming since 1985 with an average rate of 0.045 ± 0.011 °C/year and with the highest rate of 0.10 ± 0.01 °C/year [32]. There has been an observed increasing trend mean annual air temperature in the Selenga River basin by 1.4 °C or 0.036 °C/year during the considered historical period from 1979 to 2016 ($p < 0.05$). This is almost twice as much as the global average warming rate of 0.012 °C/year (0.72 °C increase during the period from 1951 to 2012). The climate of the Mongolian's Selenga river basin is characterized by long and cold winters, dry and hot summers, less precipitation, and high-temperature fluctuations [10,33]. The annual mean precipitation is 300–400 mm/year in the Khangai, Khentein, and Huvsgul mountainous regions 150–250 mm/year in the steppe and river valleys. The results of this study are generally consistent with other research results which reported increased air temperature and changes precipitation [33,34].

The Selenga River basin lies in the zone of extremely continental climate and a considerable portion of the basin is occupied by permafrost [10]. Runoff formation conditions in the Selenga River basin are very diverse. The southern part of the Selenga River basin shows low soil moisture content and steppe vegetation, while its northern part is covered by dense taiga vegetation and permafrost—an important source of soil water in summer. The high elevation difference (from 418 to 3514 m) also has its effect on runoff formation conditions. Rains are the main source of Selenga River basin nourishment. Snow cover in its drainage basin is not rich, hence the low share of snow in river nourishment. About half of Selenga annual runoff is the runoff occurred in summer season (June–August), the role of groundwater in river nourishment is also small [35]. Selenga river basin runoff varies mostly because of variations of summer precipitation. The rivers of the Selenga River basin show pronounced winter low-water period from November to March (3–10% of the annual runoff volume), a relatively low spring snow-melt flood and a series of rain floods in summer and autumn. Many rivers freeze in the winter season [36]. Especially hydrological processes are very sensitive. The MK, ITAM, and Sen's slope estimator test analysis showed that decreasing trend of river discharge was observed across the stations. The river discharge has a sharp decreasing trend significantly since 1995. It is maybe related to the impact of other factors. Especially, this may be due to the socioeconomic activities including mining, industry, agriculture, and urbanization in the basin [8,37–40].

5. Conclusions

In this study, the Mann–Kendall trend test, ITAM, and Sen's slope estimator test methods were used to analyze the variability of precipitation, air temperature, and river discharge on an annual basis in the study basin.

Seasonal variability of precipitation was investigated in all stations. The small significant increasing trend was observed in Ulaanbaatar, Erdenet, and Tsetserleg stations, whereas other Murun and Sukhbaatar stations demonstrated a significant increasing trend. The average annual air temperature for Mongolian's Selenga river basin is 0.83 °C. The average air temperature has significantly increased by 1.4 °C in the past 38 years. This is very high in the semi-arid zone of central Asia during the past 40 years. This is almost twice the global average warming rate. The river discharge trend has significantly decreased in the determined study periods. It has been particularly apparent since 1995. There was conformity in the results obtained from the Mann–Kendall, ITAM test, Sen's slope estimator test and the trend line for all stations during the specified study period.

In the near future, it's vital to conduct scientific studies on the causes of river discharge change and its potential influences on the Ecohydrological systems in the basin area.

Author Contributions: B.D. made substantial contributions to the design, idea generating, analysis, interpretation, and drafting of the manuscript. Y.D. assisted and commented on the draft manuscript and supervised the whole work. W.H. advising and operated the MK test for data analysis and is a resource person. S.C. and A.E. interpreted the results. X.Y., M.G., A.A. and A.G. are participated in the design of the study and supervised all methodologies utilized. The final manuscript before submission was checked and approved by all the authors.

Funding: This research was funded by The China, National Key Research and Development Project (grant No. 2016YFA0601503).

Acknowledgments: The authors would like to thank the Information and Research Institute of Meteorology, Hydrology, and Environment of Mongolian for providing the raw meteorological data. We also thank the China Institute of Water Resources and Hydropower Research for financing this research.

Conflicts of Interest: The authors declare no conflict of interest.

References

1. Palmate, S.S.; Pandey, A.; Kumar, D.; Pandey, R.P.; Mishra, S.K. Climate change impact on forest cover and vegetation in Betwa Basin, India. *Appl. Water Sci.* **2017**, *7*, 103–114. [[CrossRef](#)]
2. Malsy, M.; Aus der Beek, T.; Eisner, S.; Flörke, M. Climate change impacts on Central Asian water resources. *Adv. Geosci.* **2012**, *32*, 77–83. [[CrossRef](#)]
3. Malsy, M.; Flörke, M.; Borchart, D. What drives the water quality changes in the Selenga Basin: Climate change or socio-economic development? *Reg. Environ. Chang.* **2017**, *17*, 1977–1989. [[CrossRef](#)]
4. Kayet, N.; Pathak, K.; Chakrabarty, A.; Sahoo, S. Spatial impact of land use/land cover change on surface temperature distribution in Saranda Forest, Jharkhand. *Model. Earth Syst. Environ.* **2016**, *2*, 127. [[CrossRef](#)]
5. Zhuo, L.; Han, D.; Dai, Q. Exploration of empirical relationship between surface soil temperature and surface soil moisture over two catchments of contrasting climates and land covers. *Arabian J. Geosci.* **2017**, *10*, 410. [[CrossRef](#)]
6. Wang, G.; Zhang, J.; Li, X.; Bao, Z.; Liu, Y.; Liu, C.; He, R.; Luo, J. Investigating causes of changes in runoff using hydrological simulation approach. *Appl. Water Sci.* **2017**, *7*, 2245–2253. [[CrossRef](#)]
7. Walling, D.E.; Fang, D. Recent trends in the suspended sediment loads of the world's rivers. *Glob. Planet. Chang.* **2003**, *39*, 111–126. [[CrossRef](#)]
8. Ma, X.; Yasunari, T.; Ohata, T.; Natsagdorj, L.; Davaa, G.; Oyunbaatar, D. Hydrological regime analysis of the Selenge River basin, Mongolia. *Hydrol. Process.* **2003**, *17*, 2929–2945. [[CrossRef](#)]
9. Fang, J.; Bai, Y.; Wu, J. Towards a better understanding of landscape patterns and ecosystem processes of the Mongolian Plateau. *Landsc. Ecol.* **2015**, *30*, 1573–1578. [[CrossRef](#)]
10. Törnqvist, R.; Jarsjö, J.; Pietroń, J.; Bring, A.; Rogberg, P.; Asokan, S.M.; Destouni, G. Evolution of the hydro-climate system in the Lake Baikal basin. *J. Hydrol.* **2014**, *519*, 1953–1962. [[CrossRef](#)]
11. Karthe, D.; Chalov, S.; Moreido, V.; Pashkina, M.; Romanchenko, A.; Batbayar, G.; Kalugin, A.; Westphal, K.; Malsy, M.; Flörke, M. Assessment of runoff, water and sediment quality in the Selenga River basin aided by a web-based geoservice. *Water Resour.* **2017**, *44*, 399–416. [[CrossRef](#)]
12. Kasimov, N.; Karthe, D.; Chalov, S. Environmental change in the Selenga River—Lake Baikal Basin. *Reg. Environ. Chang.* **2017**, *17*, 1945–1949. [[CrossRef](#)]
13. Troitskaya, E.; Blinov, V.; Ivanov, V.; Zhdanov, A.; Gnatovsky, R.; Sutyryna, E.; Shimaraev, M. Cyclonic circulation and upwelling in Lake Baikal. *Aquat. Sci.* **2015**, *77*, 171–182. [[CrossRef](#)]
14. United Nations Development Programme (UNDP). Chapter I. General Characteristics of Lake Baikal Basin. In *State of the Environment Report. The Lake Baikal Basin 2012–2013*; United Nations Development Programme: New York, NY, USA, 2013.
15. Moore, M.V.; Hampton, S.E.; Izmes't'eva, L.R.; Silov, E.A.; Peshkova, E.V.; Pavlov, B.K. Climate Change and the World's "Sacred Sea"—Lake Baikal, Siberia. *BioScience* **2009**, *59*, 405–417. [[CrossRef](#)]
16. United Nations Educational, Scientific and Cultural Organization (UNESCO). *Convention Concerning the Protection of the World Cultural and Natural Heritage*; Report; United Nations Educational, Scientific and Cultural Organization: Paris, France, 1996. Available online: <http://whc.unesco.org/archive/repcom96.htm#754> (accessed on 10 March 1997).

17. Sharma, K.P.; Moore, B.; Vorosmarty, C.J. Anthropogenic, Climatic, and Hydrologic Trends in the Kosi Basin, Himalaya. *Clim. Chang.* **2000**, *47*, 141–165. [[CrossRef](#)]
18. Déry, S.J.; Wood, E.F. Decreasing river discharge in northern Canada. *Geophys. Res. Lett.* **2005**, *32*. [[CrossRef](#)]
19. McClelland, J.W.; Déry, S.J.; Peterson, B.J.; Holmes, R.M.; Wood, E.F. A pan-arctic evaluation of changes in river discharge during the latter half of the 20th century. *Geophys. Res. Lett.* **2006**, *33*. [[CrossRef](#)]
20. Asfaw, A.; Simane, B.; Hassen, A.; Bantider, A. Variability and time series trend analysis of rainfall and temperature in northcentral Ethiopia: A case study in Woleka sub-basin. *Weather Clim. Extremes* **2018**, *19*, 29–41. [[CrossRef](#)]
21. Gedefaw, M.; Yan, D.; Wang, H.; Qin, T.; Girma, A.; Abiyu, A.; Batsuren, D. Innovative Trend Analysis of Annual and Seasonal Rainfall Variability in Amhara Regional State, Ethiopia. *Atmosphere* **2018**, *9*, 326. [[CrossRef](#)]
22. Wu, L.; Wang, S.; Bai, X.; Luo, W.; Tian, Y.; Zeng, C.; Luo, G.; He, S. Quantitative assessment of the impacts of climate change and human activities on runoff change in a typical karst watershed, SW China. *Sci. Total Environ.* **2017**, *601–602*, 1449–1465. [[CrossRef](#)] [[PubMed](#)]
23. Ma, X.; He, Y.; Xu, J.; van Noordwijk, M.; Lu, X. Spatial and temporal variation in rainfall erosivity in a Himalayan watershed. *CATENA* **2014**, *121*, 248–259. [[CrossRef](#)]
24. Wu, H.S.; Liu, D.F.; Chang, J.X.; Zhang, H.X.; Huang, Q. Impacts of climate change and human activities on runoff in Weihe Basin based on Budyko hypothesis. *IOP Conf. Ser. Earth Environ. Sci.* **2017**, *82*, 012063. [[CrossRef](#)]
25. Wu, H.; Qian, H. Innovative trend analysis of annual and seasonal rainfall and extreme values in Shaanxi, China, since the 1950s. *Int. J. Climatol.* **2017**, *37*, 2582–2592. [[CrossRef](#)]
26. Cui, L.; Wang, L.; Lai, Z.; Tian, Q.; Liu, W.; Li, J. Innovative trend analysis of annual and seasonal air temperature and rainfall in the Yangtze River Basin, China during 1960–2015. *J. Atmos. Sol. Terr. Phys.* **2017**, *164*, 48–59. [[CrossRef](#)]
27. Gocic, M.; Trajkovic, S. Analysis of changes in meteorological variables using Mann-Kendall and Sen’s slope estimator statistical tests in Serbia. *Glob. Planet. Chang.* **2013**, *100*, 172–182. [[CrossRef](#)]
28. Gu, X.; Zhang, Q.; Singh, V.P.; Shi, P. Changes in magnitude and frequency of heavy precipitation across China and its potential links to summer temperature. *J. Hydrol.* **2017**, *547*, 718–731. [[CrossRef](#)]
29. St Laurent, J.; Mazumder, A. Influence of seasonal and inter-annual hydro-meteorological variability on surface water fecal coliform concentration under varying land-use composition. *Water Res.* **2014**, *48*, 170–178. [[CrossRef](#)] [[PubMed](#)]
30. Wang, H.; Zhang, M.; Zhu, H.; Dang, X.; Yang, Z.; Yin, L. Hydro-climatic trends in the last 50years in the lower reach of the Shiyang River Basin, NW China. *CATENA* **2012**, *95*, 33–41. [[CrossRef](#)]
31. Sorg, A.; Bolch, T.; Stoffel, M.; Solomina, O.; Beniston, M. Climate change impacts on glaciers and runoff in Tien Shan (Central Asia). *Nat. Clim. Change* **2012**, *2*, 725. [[CrossRef](#)]
32. Li, X.; Zhang, L.; Yang, G.; Li, H.; He, B.; Chen, Y.; Tang, X. Impacts of human activities and climate change on the water environment of Lake Poyang Basin, China. *Geoenvirom. Disasters* **2015**, *2*, 22. [[CrossRef](#)]
33. Batima, P.; Natsagdorj, L.; Gombluudev, P.; Erdenetsetseg, B. Observed Climate Change in Mongolia. *AIACC Work. Pap.* **2005**, *12*, 1–26.
34. Nandintsetseg, B.; Greene, J.S.; Goulden, C.E. Trends in extreme daily precipitation and temperature near lake Hövsgöl, Mongolia. *Int. J. Climatol.* **2007**, *27*, 341–347. [[CrossRef](#)]
35. Bereznykh, T.V.; Marchenko, O.Y.; Abasov, N.V.; Mordvinov, V.I. Changes in the summertime atmospheric circulation over East Asia and formation of long-lasting low-water periods within the Selenga river basin. *Geogr. Nat. Resour.* **2012**, *33*, 223–229. [[CrossRef](#)]
36. Frolova, N.L.; Belyakova, P.A.; Grigor’ev, V.Y.; Sazonov, A.A.; Zotov, L.V. Many-year variations of river runoff in the Selenga basin. *Water Resour.* **2017**, *44*, 359–371. [[CrossRef](#)]
37. Chalov, S.R.; Jarsjö, J.; Kasimov, N.S.; Romanchenko, A.O.; Pietroń, J.; Thorslund, J.; Promakhova, E.V. Spatio-temporal variation of sediment transport in the Selenga River Basin, Mongolia and Russia. *Environ. Earth Sci.* **2015**, *73*, 663–680. [[CrossRef](#)]
38. Stubblefield, A.; Chandra, S.; Eagan, S.; Tuvshinjargal, D.; Davaadorzh, G.; Gilroy, D.; Sampson, J.; Thorne, J.; Allen, B.; Hogan, Z. Impacts of gold mining and land use alterations on the water quality of central Mongolian rivers. *Integr. Environ. Assess. Manag.* **2005**, *1*, 365–373. [[CrossRef](#)] [[PubMed](#)]

39. Sorokovikova, L.M.; Popovskaya, G.I.; Tomberg, I.V.; Sinyukovich, V.N.; Kravchenko, O.S.; Marinaite, I.I.; Bashenkhaeva, N.V.; Khodzher, T.V. The Selenga River water quality on the border with Mongolia at the beginning of the 21st century. *Russ. Meteorol. Hydrol.* **2013**, *38*, 126–133. [[CrossRef](#)]
40. Karthe, D.; Heldt, S.; Houdret, A.; Borchardt, D. IWRM in a country under rapid transition: Lessons learnt from the Kharaa River Basin, Mongolia. *Environ. Earth Sci.* **2015**, *73*, 681–695. [[CrossRef](#)]



© 2018 by the authors. Licensee MDPI, Basel, Switzerland. This article is an open access article distributed under the terms and conditions of the Creative Commons Attribution (CC BY) license (<http://creativecommons.org/licenses/by/4.0/>).